ELSEVIER

International Journal of Inorganic Materials 2 (2000) 53–59

International Journal of Inorganic Materials

Structure and magnetism in Pr_3RuO_7

Frederick Wiss, N.P. Raju, A.S. Wills, J.E. Greedan*

Brockhouse Institute for Materials Research and Department of Chemistry, McMaster University, Hamilton, Canada L8S 4M1

Received 10 November 1999; accepted 16 November 1999

Abstract

The crystal structure of the ordered fluorite, Pr_3RuO_7, was refined from powder neutron diffraction data in *Cmcm*. An interesting structural feature is the presence of relatively well separated zig-zag chains of corner sharing RuO_6 octahedra, Ru–Ru interchain distance 6.61 Å vs. Ru–Ru intrachain distance of 3.76 Å. Magnetic susceptibility data show a Curie–Weiss behavior for $T>225$ K with $C=5.96(4)$ emu K mol^{-1} and $\theta_c=+11(2)$ K. In an attempt to separate the contributions of Pr(3+) and Ru(5+), the properties of isostructural Pr_3TaO_7 were also measured, yielding $C=4.63(3)$ emu K mol^{-1}. Thus, the contribution of Ru(5+), $4d^3$, $S=3/2$, to the measured Curie constant is estimated to be 1.33 emu K mol^{-1}, not far from the spin-only value of 1.87 emu K mol^{-1}. This supports the view that the Ru 4*d* electrons are localized and magnetic, not itinerant. A susceptibility maximum at about 50 K is attributed to long-range magnetic order and this is substantiated by neutron diffraction data. There is little evidence for one-dimensional antiferromagnetic correlations in this material but behavior characteristic of short-range ferromagnetic correlations attributed to Pr–Ru exchange interactions are found in the temperature range 50–200 K, consistent with the positive θ_c.

Keywords: A. oxides; B. chemical synthesis; C. neutron scattering; C. X-ray diffraction; D. magnetic properties

1. Introduction

Oxides of composition A_3BO_7, where A is usually a lanthanide and B is pentavalent, crystallize in a structure which can be described as an ordered variant of cubic fluorite, AO_2. In this case the cations, which are of significantly different radii, order in a $2_A{:}1_A{:}1_B$ pattern over the f.c.c. fluorite cation sites. As well, the oxygen vacancies, required by charge neutrality, also order. The resulting unit cell is orthorhombic with dimensions $a_0=\sqrt{2}a_F$, $b_0=\sqrt{2}a_F$ and $c_0=2a_F$. The pentavalent B cation is octahedrally coordinated and the octahedra share corners forming a zig-zag chain parallel to the *c*-axis in the most commonly chosen setting (Fig. 1). The interchain B–B distance is about 6.6 Å compared to the corresponding intrachain distance of 3.7 Å. This suggests that materials which crystallize in this structure type may exhibit one-dimensional electronic behavior. This ordered structure is known for B=Nb, Ta, Sb, Mo, Ru, Re and Ir for the larger

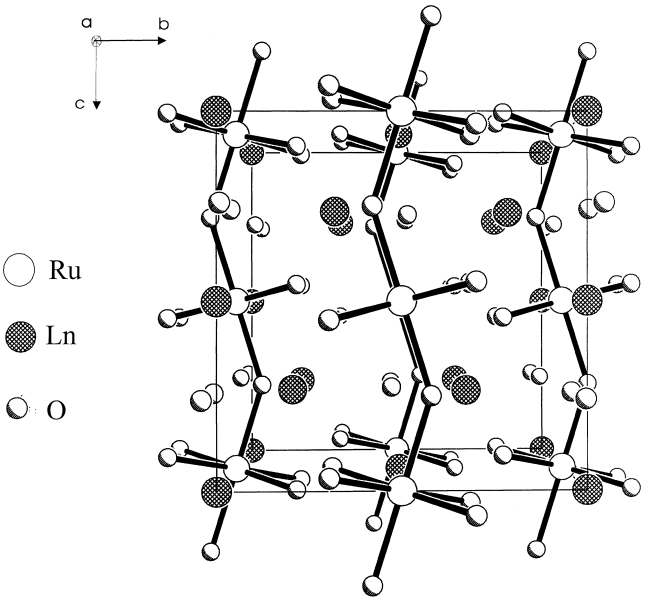

Fig. 1. The crystal structure of the orthorhombic ordered fluorite A_3BO_7, illustrated by Ln_3RuO_7.

*Corresponding author.

1466-6049/00/$ – see front matter
PII: S1466-6049(99)00065-3

lanthanides, A = La–Eu, while for the smaller A ions, Gd–Y, a disordered fluorite structure, obtains [1–13]. A variety of space groups have been reported for the ordered phase. For the ruthenates, *Cmcm* appears to provide a good description while La_3MoO_7 was solved in $P2_12_12_1$ [7,12]. Of the known materials those for which B = Mo($4d^1$), Ru($4d^3$), Re($5d^2$) or Ir($5d^4$) are of interest for B-site electronic properties. Recently, La_3MoO_7 has been shown to be a semiconductor with quite complex magnetic properties [12]. A broad susceptibility maximum at about 655 K was interpreted as evidence for strong, $J/k = -511$ K, intrachain antiferromagnetic correlations and a sharp decrease below 140 K was taken as evidence for possible long-range magnetic order. There is supporting, but not definitive, evidence for the latter from powder neutron diffraction data. There have been relatively few other studies of physical properties in this class of materials; for example, Nd_3IrO_7 was reported to be semiconducting [8]. As well, magnetic properties have been measured for several Pr_3BO_7 phases where B is Nb, Ta or Sb [9]. Very recently, La_3RuO_7 has been characterized [13]. The material is semiconducting and shows evidence of antiferromagnetic Ru–Ru spin–spin coupling, $\theta_c = -14$ K, with short-range antiferromagnetic correlations in the range 20–50 K and long-range antiferromagnetic order below 17 K. The Ru–O–Ru angle along the chains of corner sharing octahedra is 145°. The results presented here concern Pr_3RuO_7, which has not been reported before, obtained as part of a more comprehensive study of the Ln_3RuO_7 series.

2. Experimental

2.1. Sample preparation

The following reaction was used:

$$3Pr_2O_3 + 2RuO_2 + (1/2)O_2 \rightarrow 2Ln_3RuO_7$$

Pr_2O_3 was prepared from Pr_6O_{11}, Rhone-Poulenc, 99.99% by firing under H_2 gas at 900°C for 48 h. RuO_2 was obtained from Cerac, 99.99%. Powders of the starting compounds were mixed under acetone in an agate mortar and pestle, pressed into pellets, wrapped in platinum foil and loaded into a quartz tube. The oxygen was provided by a weighed pellet of CrO_3 which was also wrapped in platinum foil and enclosed in the reaction tube. The tube was evacuated to about 10^{-5} Torr and sealed. The tube was fired at 1050°C for 48 h.

Pr_3TaO_7 was prepared by reaction of Pr_6O_{11} and Ta_2O_5 (Cerac, 99.9%) fired in air at 1350°C for 96 h.

2.2. X-ray powder diffraction

Phase purity was monitored by powder X-ray diffraction using a Guinier–Hagg camera with CuKα_1 radiation, $\lambda = 1.54056$ Å and an internal silicon standard. The Guinier films were read with a computer-controlled LS-20 line scanner (KEJ Instruments, Taby, Sweden) and the data analysed using the software system LSUDF.

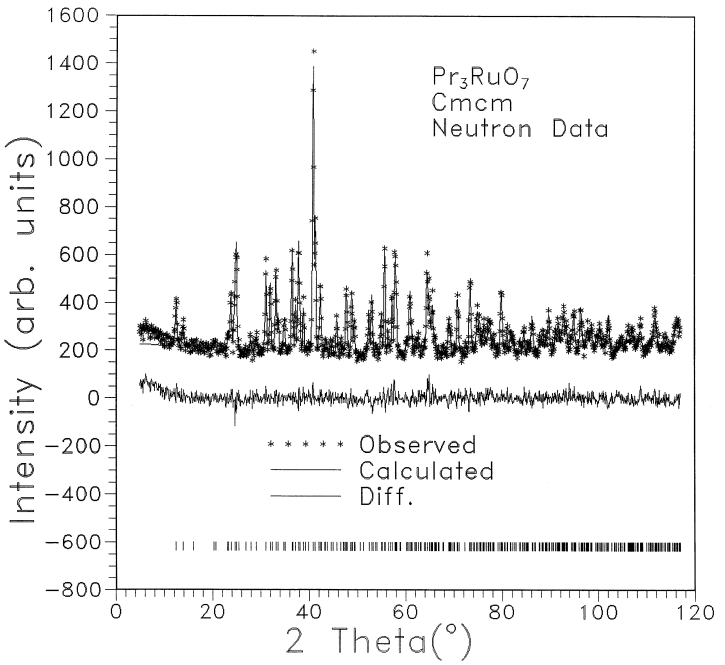

Fig. 2. Rietveld refinement of neutron powder diffraction data for Pr_3RuO_7. The crosses represent the data, the solid line the calculated profile and the lower line the difference pattern. The vertical tic marks locate the Bragg peaks.

Table 1
Refined unit cell, atomic position and displacement parameters for Pr_3RuO_7 from powder neutron diffraction data[a]

Space group: *Cmcm*
$Z=4$
$a=10.974(1)$ Å
$b=7.3908(7)$ Å
$c=7.5239(7)$ Å

Atom	*x*	*y*	*z*	*B* (Å^2)
Pr1(4a)	0	0	0	0.42(20)
Pr2(8g)	0.22224(69) [0.2226(3)]	0.3132(11) [0.3093(4)]	0.25	0.46(13)
Ru(4b)	0	0.5	0	0.61(16)
O1(16h)	0.12532(42) [0.1257(3)]	0.31800(66) [0.3169(4)]	−0.04188(66) [−0.0412(4)]	0.81(8)
O2(8g)	0.13099(66) [0.1309(4)]	0.03297(81) [0.0278(6)]	0.25	0.34(11)
O3(4c)	0	0.41913(117) [0.4168(7)]	0.25	0.53(17)

[a] The [ ] indicate corresponding values for Nd_3RuO_7 [7]. $R_p=0.0607$, $R_{wp}=0.0757$, $R_I=0.0896$, $R_E=0.0614$, $\chi^2=1.52$.

2.3. Neutron powder diffraction

Neutron powder diffraction data were obtained both at the McMaster Nuclear Reactor using $\lambda=1.3920$ Å neutrons and at DUALSPEC, operated by the Neutron Program for Materials Research of the National Research Council of Canada at the Chalk River laboratories using $\lambda=1.32637$ Å neutrons at a variety of temperatures. The samples were contained in either aluminum or vanadium cans sealed under helium using an indium wire seal. For the McMaster experiments the temperature was controlled using a closed-cycle refrigerator. The data were refined using the software package FULLPROF [14].

2.4. Magnetic measurements

Magnetic susceptibility data for Pr_3RuO_7 were obtained with a SQUID magnetometer (Quantum Design) over the temperature range 5–350 K at a low applied field of 500 Oe.

3. Results and discussion

The Guinier powder X-ray data indicated that the sample was single phase and that the unit cell was orthorhombic with cell constants, $a=10.9730(9)$ Å, $b=7.3889(7)$ Å and $c=7.5251(8)$ Å. A total of 39 reflections were observed all of which appeared to be consistent with the C-centering condition, $h+k=2n$.

Based on the observation above and the model for Nd_3RuO_7 [7], a room-temperature neutron diffraction data set (DUALSPEC) was refined. The results are shown in Fig. 2 and Tables 1 and 2. The refinement in *Cmcm* is seen to be successful.

The distances and angles are in excellent agreement with those determined for Nd_3RuO_7 and the unit cell constants are consistent with those determined from X-ray Guinier data.

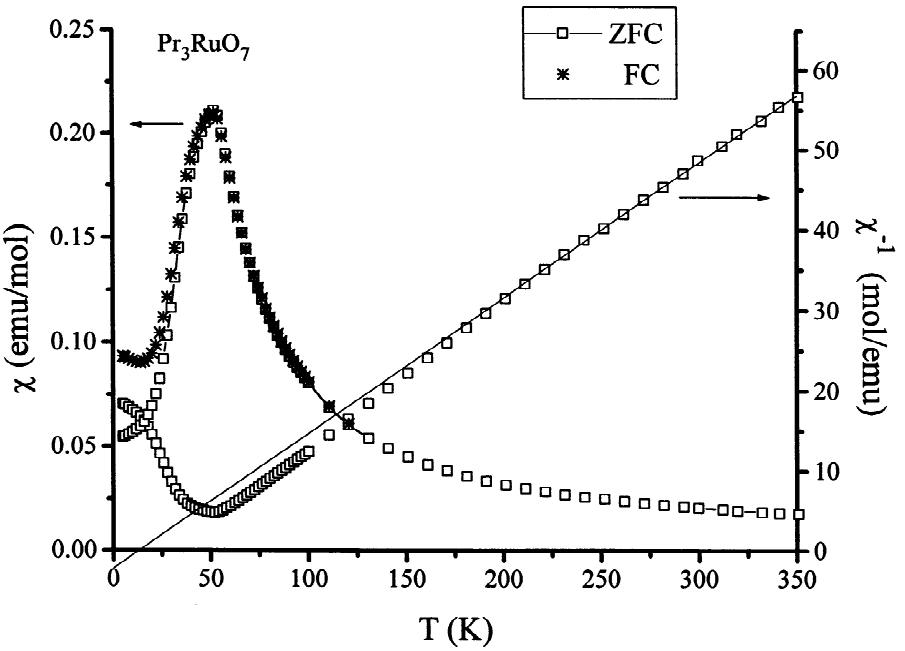

Fig. 3. Magnetic susceptibility (left axis) and inverse susceptibility (right axis) data for Pr_3RuO_7.

Table 2
Selected bond distances (Å) and angles (°) for Pr_3RuO_7[a]

Pr1–O1	2.741(5)	4*x*	[2.729(3)]	Ru–O1	1.949(5)	4*x*	[1.950(3)]
Pr1–O2	2.380(4)	4*x*	[2.365(3)]	Ru–O3	1.974(3)	2*x*	[1.972(2)]
Pr2–O1	2.440(6)	2*x*	[2.461(4)]	Ru–O3–Ru	144.7(5)		[143.7(3)]
Pr2–O1	2.488(8)	2*x*	[2.426(3)]	O1–Ru–O3	86.85(22)		[86.3(1)]
Pr2–O2	2.300(10)	1*x*	[2.306(5)]	O1–Ru–O1	89.74(20)		[89.34(9)]
Pr2–O2	2.288(10)	1*x*	[2.270(5)]				
Pr2–O3	2.561(8)	1*x*	[2.554(4)]				

[a] The values in [ ] are the corresponding ones for Nd_3RuO_7.

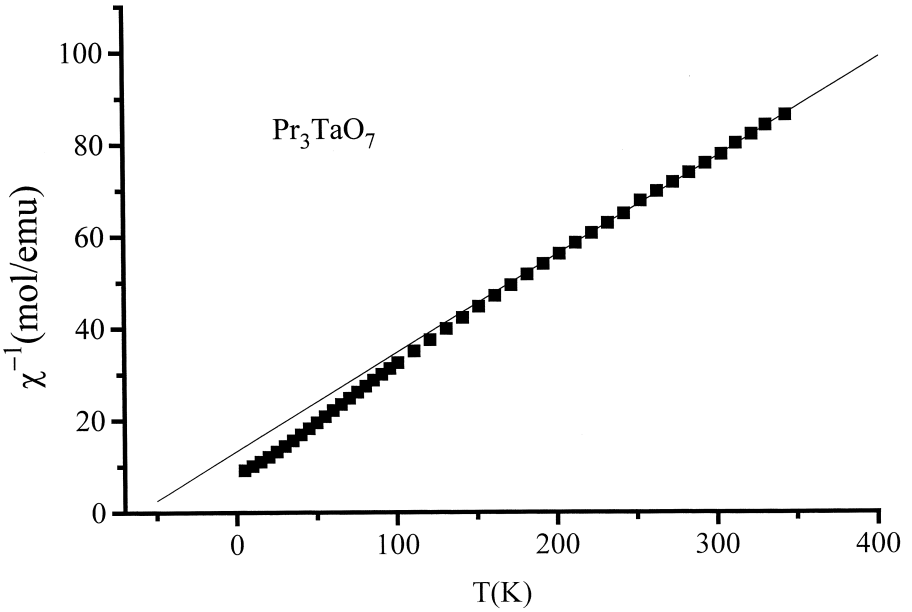

Fig. 4. Inverse magnetic susceptibility data for Pr_3TaO_7.

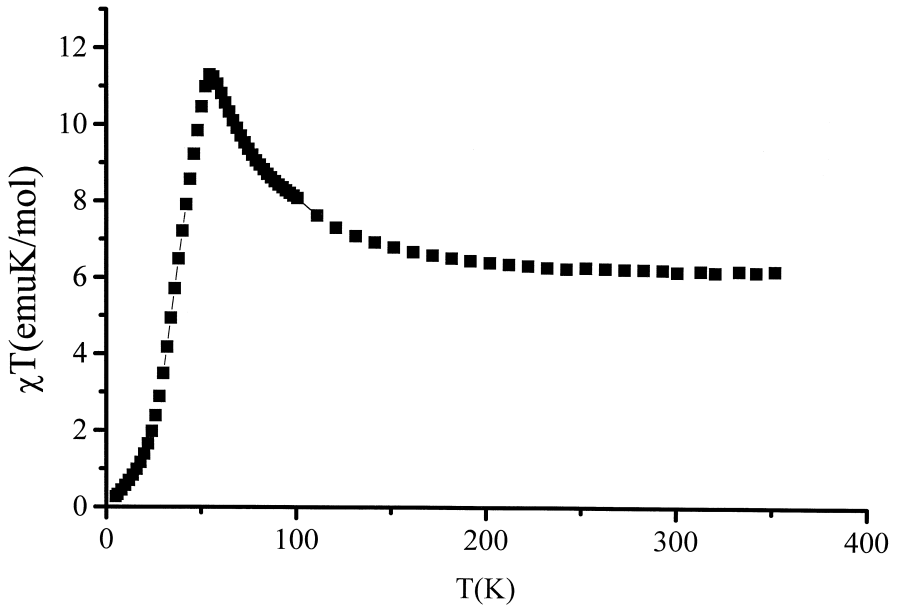

Fig. 5. χT vs. T for Pr_3RuO_7 showing evidence for short-range ferromagnetic correlations.

3.1. Magnetic properties

The magnetic susceptibility data for Pr_3RuO_7 are shown in Fig. 3. The Curie–Weiss regime is seen only at relatively high temperatures, $T>225$ K. The derived constants are $C=5.96(4)$ emu K mol^{-1} and $\theta_c=+11(2)$ K. It is of course somewhat difficult to interpret the Curie constant as it consists of contributions from Pr(3+) at both sites and Ru(5+), i.e. $C_{obs}=C(Pr[1])+2C(Pr[2])+C(Ru)$. In order to isolate the Ru(5+) contribution, data were obtained for the isostructural Pr_3TaO_7, where Ta(5+) is diamagnetic. These results are given in Fig. 4, where the Curie–Weiss law also obtains, apparently, for $T>225$ K, yielding $C=4.633$ emu K mol^{-1} and $\theta_c=-60(2)$ K. Assuming that this compound models well the contributions C(Pr[1]) and C(Pr[2]), then, the value for C(Ru) is 1.33(7) emu K mol^{-1}. This can be compared to a spin-only value for an $S=3/2$ system of 1.87 emu K mol^{-1} or comparing effective moments, 3.26 BM vs. 3.87 BM. The agreement is seen to be reasonable given the assumptions involved

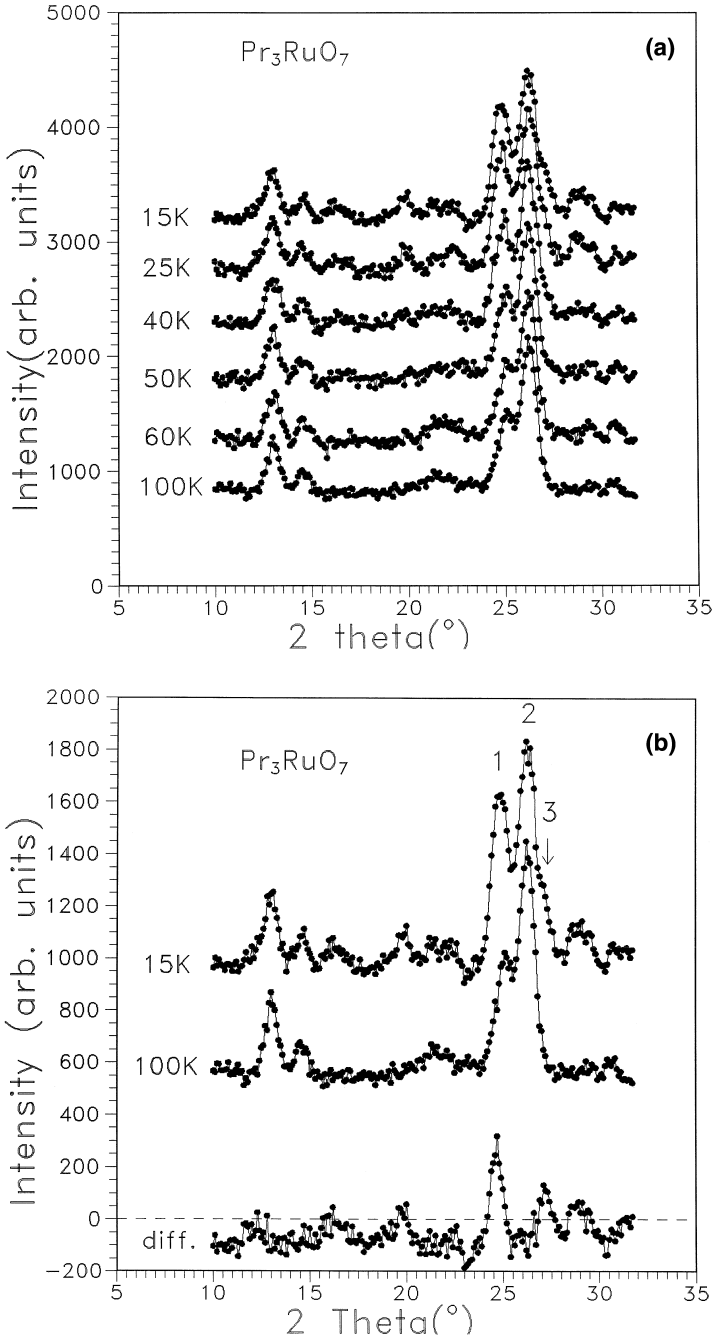

Fig. 6. (a) Low-angle neutron powder diffraction data for Pr_3RuO_7 at selected temperatures from 15 K to 100 K. (b) Comparison of neutron powder diffraction data for Pr_3RuO_7 at 15 K and 100 K and the difference pattern. Three reflections are marked as peaks 1, 2 and 3.

and this result supports a localized electron picture for Ru(5+).

That θ_c is positive for the Ru phase and negative for the tantalum material also requires comment. For Pr_3TaO_7 there are two contributions to the observed θ_c, one due to Pr–Pr exchange and one to the so-called crystal field contribution. The Pr–Pr exchange contribution is presumably weak as there is no evidence from Fig. 4 of magnetic long-range or short-range order down to 5 K. The appearance of a positive θ_c for Pr_3RuO_7 then implies ferromagnetic Pr–Ru or Ru–Ru interactions. It is known that θ_c for La_3RuO_7 is negative [13], i.e. that Ru–Ru is negative, which suggests that the Pr–Ru exchange must be positive. Useful information is available from Fig. 5 in which the product χT is plotted vs. T. Clear evidence for short-range ferromagnetic order is seen in the upturn in χT which begins gradually at about 200 K and accelerates below 100 K.

As seen from Figs. 3 and 5, there is also clear evidence for antiferromagnetism below 50 K. The divergence in field-cooled vs. zero-field-cooled data at about 25 K may indicate the onset of some form of spin-canting.

Neutron diffraction data [Fig. 6(a) and (b)] support the onset of long-range antiferromagnetic order. From Fig. 6(a), several new reflections develop below about 50 K. This is more clearly seen in Fig. 6(b), where the data for 15 K and 100 K are compared along with a difference plot. That the background for the difference data is negative supports the assignment of this new scattering to magnetic origins. This results from the fact that the paramagnetic neutron scattering, which is greatest at low angles and is incoherent at 100 K, is missing in the long-range ordered state attained at 15 K, it having been 'reassigned' to the Bragg peaks. A critical temperature of about 50 K is confirmed from the data of Fig. 7, in which the temperature dependence of the three reflections indicated on Fig. 6(b) is shown. It is clear that Peak 2 is purely structural in origin while Peak 1 has both a magnetic and structural contribution, and Peak 3 is purely magnetic.

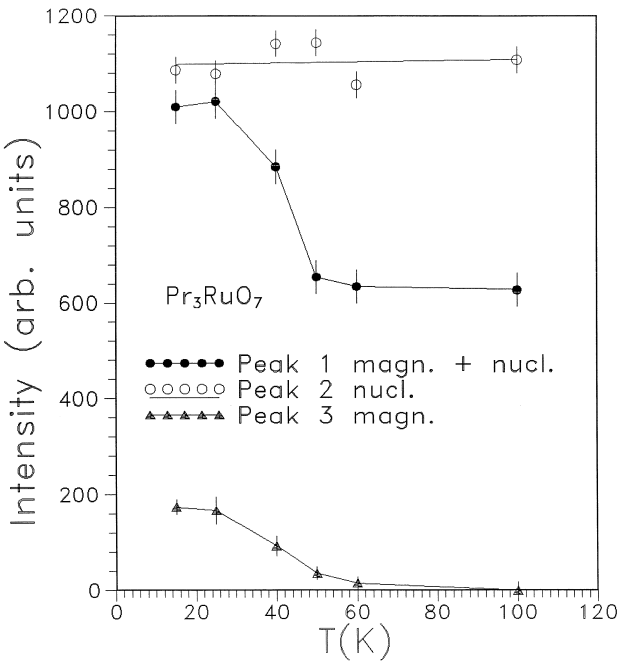

Fig. 7. The temperature dependence of the integrated intensities for the three reflections, 1, 2 and 3 identified in Fig. 6(b).

Recently, high-resolution neutron diffraction data have been obtained at low temperatures. It has been possible to establish the ordering wave vector, $\hat{k}=(1/2\ 1/2\ 1/2)$, and efforts are ongoing to solve the magnetic structure.

4. Summary

The ordered fluorite, Pr_3RuO_7 has been synthesized for the first time and its crystal structure has been refined in *Cmcm*. The structural details are, not surprisingly, similar to those for Nd_3RuO_7, reported previously. The magnetic properties, also reported for the first time, are quite complex. From the paramagnetic regime it is possible to assign an effective magnetic moment to Ru(5+) which is just slightly reduced from the spin-only value, suggesting localized electrons at this site. There is strong evidence for short-range ferromagnetic correlations which set in at relatively high temperatures, 200 K, which have been assigned, tentatively, to Pr–Ru exchange interactions. Unlike La_3MoO_7 and La_3RuO_7 this compound shows no evidence for one-dimensional antiferromagnetic correlations. Long-range antiferromagnetic order, $T_N=50$ K, is seen at low temperatures. Efforts are ongoing to determine the magnetic structures of this and other members of the Ln_3RuO_7 series.

Acknowledgements

This work was supported by the Natural Science and Engineering Research Council of Canada in the form of a Research Grant to J.E.G. We acknowledge the assistance of R. Donaberger and I. Swainson of the NPMR of NRC and the Chalk River laboratories for assistance with neutron diffraction. F. Wiss is grateful to the Conseil Regional d'Alsace for financial support.

References

[1] Tilloca G, Perez y Jorba M, Queyroux F. CR Acad Sci Paris 1970;C271:134.
[2] Allpress JG, Rossell HJ. J Solid State Chem 1979;27:105.
[3] Rossell HJ. J Solid State Chem 1979;27:115.
[4] Czeskleba-Kerner H, Cros B, Tourne G. J Solid State Chem 1981;37:294.
[5] Prevost-Czeskleba H. J Less-Common Metals 1987;127:117.
[6] van Berkel FPF, Ijdo DJW. Mat Res Bull 1986;21:1103.

[7] Groen WA, van Berkel FPF, Ijdo DJW. Acta Crystallogr 1987;C43:2262.
[8] Vente JF, Ijdo DJW. Mat Res Bull 1991;26:1255.
[9] Vente JF, Helmboldt RB, Ijdo DJW. J Solid State Chem 1994;108:18.
[10] Kahn-Harari A, Mazerolles L, Michel D, Robert F. J Solid State Chem 1995;116:103.
[11] Wltschek G, Paulus H, Svoboda I, Ehrenberg H, Fuess H. J Solid State Chem 1996;125:1.
[12] Greedan JE, Raju NP, Wegner A, Gougeon P, Padiou J. J Solid State Chem 1997;129:320.
[13] Khalifah P, Erwin RW, Lynn JW, Huang Q, Batlogg B, Cava RJ. Phys Rev 1999;B60:9573.
[14] Rodriguez-Carvajal J. FULLPROF: Rietveld, profile matching and integrated intensities refinement of X-ray and/or neutron data, Version 3.5d Oct. 98-LLB-JRC, 1998.